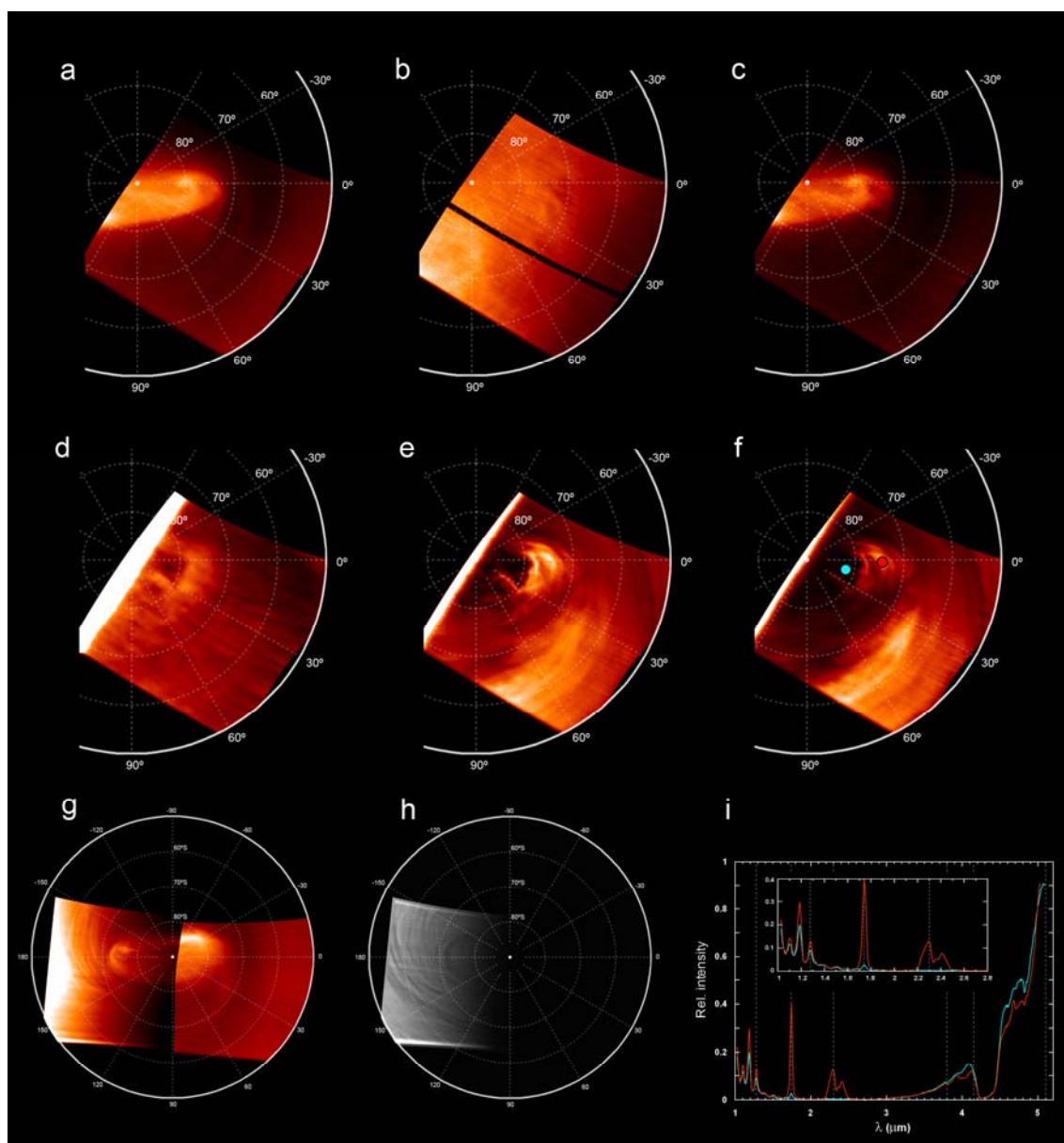


## Supplementary Figure 1: The structure of the dipole at different wavelengths.



The structure of the dipole at different wavelengths as observed on orbit 38 on the night side (panels a to f) and on orbit 29 on both night and day sides simultaneously (panels g and h). All of the images have been processed into a polar projection with the same relative size. The first row shows the structure of the upper clouds at levels close to 65 km, at three wavelengths: **a**, 5.1  $\mu\text{m}$ ; **b**, 4.15  $\mu\text{m}$ ; and **c**, 3.8  $\mu\text{m}$ . The second row shows the structure of the lower cloud at an altitude of about 50 km: **d** 1.27  $\mu\text{m}$ . **e**, 1.74  $\mu\text{m}$ . **f**, 2.3  $\mu\text{m}$ . The third row shows the structure of the dipole as seen on orbit 29: **g**,

observations at 3.8  $\mu\text{m}$  during the day (left) and at 5.1  $\mu\text{m}$  during the night (right); **h**, at 400 nm in the visible channel. Note the strong anticorrelation between the dark cloud features seen in the visible (panel h) and the bright emission regions in the infrared (panel g), in both the dipole and in the spiral arms around it. This is probably due to the optical properties of the particles: when they reflect more light from the Sun, they absorb less energy and vice versa. They may also emit less thermal IR radiance, due to the lower emissivity that would be expected to accompany the high reflectivity.

The last panel (**i**) shows spectra in adjacent regions in the dipole (the red and blue spectra correspond to the red and blue spots on panel f), with similar brightness in the thermal infrared (right side of the spectrum), but with very different radiance at both 1.74 and 2.3  $\mu\text{m}$ , explained by the different thickness of the clouds. Vertical dashed lines in panel i represent the wavelengths corresponding to the images shown in panels a to g. In the near-IR windows, the bright regions occur where the clouds are thinner, while the darker regions occur where the clouds are thicker. In some cases both windows disappeared altogether because of thick clouds, and the effective layer for emission of radiation is within the clouds at altitude higher than 50 km. Two possible reasons for this are a higher number density of particles or larger mean particle size. We note that the presence of large (mode 3) particles at high latitudes was observed earlier by Venera 15 and by Galileo NIMS. At latitudes lower than 80° south, in most areas the radiation in the near-IR windows originates in the lower atmosphere, well below the clouds.

During the observations of Mariner 10 (1972) and Pioneer Venus (1978) the north polar vortex area was cloudy, however this is not always the case. In the Venera 15 observations (1983), the haze in the north polar region was transparent in the thermal IR (the haze may even have been absent at that time) and the clouds above the north pole

had a sharp upper boundary at around 60 km. During Venus Express orbits 29 and 38 the area of the vortex appeared free of upper clouds or haze (or at least the clouds were optically thin at 5.1 and 3.8  $\mu\text{m}$ ) and the S-shape of the dipole was observed. The Rayleigh optical depth of the gaseous  $\text{CO}_2$  atmosphere above 60 km in the UV and blue channels of VIRTIS does not exceed 0.1, which means in principle the dipole structure may be observed in the UV and blue spectral regions in absence of hazes. Indeed the visibility depends on the contrast which is produced by the UV absorber or by Rayleigh scattering in the gaseous atmosphere above clouds at different altitudes. In panel g (left, 3.8  $\mu\text{m}$ , day side) and h (400 nm) a similar structure is seen in both spectral ranges. In conditions where clouds or haze occur above the polar vortex, the S-shape details of the dipole cannot be discerned, but just its overall oval shape. From the data studied so far from Venus Express VIRTIS this seems to be the most frequent condition.